New Journal of Physics
The open access journal at the forefront of physics
Deutsche Physikalische Gesellschaft DPG | IOP Institute of Physics

The solvation and ion condensation properties for sulfonated polyelectrolytes in different solvents—a computational study

J Smiatek[1,3], **A Wohlfarth**[2] **and C Holm**[1]

[1] Institut für Computerphysik, Universität Stuttgart, D-70569 Stuttgart, Germany
[2] Max-Planck-Institut für Festkörperforschung, Heisenbergstrasse 1, D-70569 Stuttgart, Germany
E-mail: smiatek@icp.uni-stuttgart.de

Received 14 August 2013, revised 6 January 2014
Accepted for publication 8 January 2014
Published 5 February 2014

New Journal of Physics **16** (2014) 025001

doi:10.1088/1367-2630/16/2/025001

Abstract

In contrast to the broad knowledge about aqueous polyelectrolyte solutions, less is known about the properties in aprotic and apolar solvents. We therefore investigate the behavior of sulfonated polyelectrolytes in sodium form in the presence of different solvents via all-atom molecular dynamics simulations. The results clearly reveal strong variations in ion condensation constants and polyelectrolyte conformations for different solvents like water, dimethyl sulfoxide (DMSO) and chloroform. The binding free energies of the solvent contacts with the polyelectrolyte groups validate the influence of different solvent qualities. With regard to the ion condensation behavior, the numerical findings show that the explicit values for the condensation constants depend on the preferential binding coefficient as derived by the evaluation of Kirkwood–Buff integrals. Surprisingly, the smallest ion condensation constant is observed for DMSO compared to water, whereas in the presence of chloroform, virtually no free ions are present, which is in good agreement to the donor number concept. In contrast to the results for the low condensation constants, the sodium conductivity in DMSO is smaller compared to water. We are able to relate this result to the observed smaller diffusion coefficient for the sodium ions in DMSO.

[3] Author to whom any correspondence should be addressed.

1. Introduction

Over the last few years, sulfonated polyelectrolytes and other polyelectrolytes have became more and more interesting as the electrolyte material for electrochemical energy conversion and storage systems such as proton-exchange-membrane-fuel cells (PEMFCs) and alkaline ion and redox-flow batteries [1–5]. They are used as separators between the electrodes since they are permeable for selective ions and mediate the electrochemical reactions taking place at the anode and cathode. The most prominent separator material for PEMFC applications is probably Nafion, a perfluoro-sulfonic acid polyelectrolyte [6]. But drawbacks like mechanical failure at higher temperature, inefficient proton-conductivity at low degrees of hydration as well as high material costs have resulted in the development of fluorine free aromatic hydro-carbon polyelectrolytes with much higher ion-exchange-capacities. The usage of extremely electron-poor poly(phenylene) backbones containing sulfone-units (—SO_2—) connecting the phenyl rings together with a high degree of sulfonic acid functionalities (—SO_3—) have recently led to polyelectrolytes with high stability and high proton conductivity [7–11]. The special design of the molecular structure (see figure 1) with the strong electron withdrawing effect of the sulfone links [7, 8] makes the phenyl rings very low in electron density and the attached sulfonic acid groups very acidic, facilitating the low condensation numbers of the counterions. A recent study on these polyelectrolytes in lithium and sodium form dissolved in different organic solvents showed conductivities so far known only for liquid salt electrolytes [5]. The large ionic conductivities can be explained by the immobilized sulfonic acid group, such that only the cations are free to move, which can be effectively described as a single-ion-conductor. These materials are of special interest for Li^+/Na^+-battery applications, where a high transference number in combination with conductivity is desired. With regard to the polyelectrolyte–ion systems, the situation is more complex, and in particular specific chemical interactions between the solvent–polymer and the solvent and the ion need to be considered to understand charge carrier dissociation and mobility. Experiments on these polyelectrolytes have focused on the ionic conductivity in several solvents like dimethylsulfoxide (DMSO), chloroform and other aprotic and polar species [5].

In terms of the desired quantities, the usage of DMSO has been shown as advantageous due to acceptable ion dissociation rates of 15–20% and resulting high ionic conductivities. To systematically analyze the ionic conductivities in various environments, several solvents with different dielectric constants and different protic and aprotic properties have been investigated. It has been found that the swelling of these polyelectrolytes and their conductivity does not heavily depend on the dielectric constant. However, the reason for this observation has not been investigated in detail so far. Experimental results have validated that several solvent-induced effects on the nanoscale and on the mesoscale significantly influence the static and dynamic behavior of polyelectrolytes in different ionic forms [5, 12, 13, 27]. The investigation of these solutions is of the most technological importance to gain a deeper knowledge about the solvation of polyelectrolytes. Broad insights will help us to understand the reasons for selectivity in polyelectrolytes and polyelectrolyte membranes for redox-flow batteries as well as transport in electrolytes for alkaline-ion batteries.

It has been known for a long time that the choice of the solvent significantly influences dissociation rates [14] as well as polyelectrolyte conformations [15]. Thus, in order to further improve such electrolytes, a detailed understanding of chemical solvent–solute interactions is a prerequisite. In contrast to the broad knowledge about aqueous polyelectrolyte solutions [15],

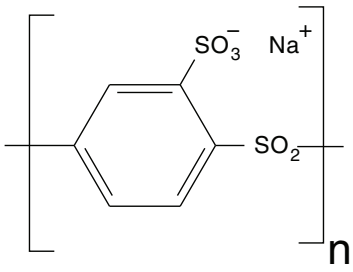

Figure 1. Chemical structure of the investigated sulfonated polyelectrolyte (mod-S220 Na^+). The degree of polymerization is $n = 9$.

less is known about polyelectrolyte properties in aprotic and apolar solvents. Atomistic simulations that focus on solvent–solute interactions by taking into account chemical details are scarce. Despite this fact, a lot of publications have focused on the influence of the solvent on polymers in a coarse-grained numerical approach or a continuum description of the solvent in theoretical attempts. The quality of the solvent for polyelectrolyte solutions in the presence of a poor solution results in surprisingly broadly varying structures compared to the globular states for uncharged polymers. For example, a decade ago, several coarse-grained simulation studies, as well as analytical attempts, proposed a pearl-necklace model for polyelectrolytes in poor solvents [15–18].

With regard to the previous attempts and results, it can be summarized that the properties of the solvent have been often modeled in a coarse-grained particle approach, which means that the detailed chemical interactions have been neglected or a continuum description was used. Thus, although the general behavior of polymers in solution due to these studies is well known, the systematic characterization of a chosen solvent concerning several properties like aprotic or protic behavior and the resulting macromolecular effects have been disregarded so far. In contrast to the small number of detailed chemical polyelectrolyte solvent studies, a large amount of biomolecular simulations that focus on the influence of water on protein or DNA structures have been published. The hydrophobic effect, as one of the main findings, has been investigated theoretically and numerically over a long time in a series of studies (see [19, 20] and references therein).

In contrast, the more general solvophobic effect, which occurs for polar species in an often apolar organic solution and vice versa, has gained much less attention [21–23]. This can be mainly explained by the biologically more-relevant investigation of macromolecular conformations in aqueous environments. A few simulation studies have focused on solvophobic effects and their influence on particle aggregation [24, 25]. It has been shown that solvophobic particles aggregate in a similar way to that observed for hydrophobic ones. However, a detailed study of enthalpic and entropic contributions, as was conducted for hydrophobic hydration [26], has yet to be performed. Furthermore, the behavior and the conformation of the often organic solvents around the solutes is largely unknown. It can be assumed that the interplay between enthalpic and entropic effects lead to important consequences for molecular behavior, as has been found in reference [5].

In addition to the molecular solvation and condensation mechanisms, another interesting point is the well-known association of highly concentrated polyelectrolytes at larger scales, which has been often observed in aqueous environments [5, 12] and investigated in terms of

the solvent polarity [28] and the counterion condensation properties [29]. The detailed reason for the occurrence and the absence of these structures in different solvents, and the influence on the ionic dissociation rates, is not clear. It has been found that the polarity of the solvent is not the main factor that influences these properties [30]. The technological benefit for an improvement of proton as well as lithium ionic conductivities as typical dissociated counterions due to favorable solvent–solute interactions and possible increased dissociation rates is of great importance. Recent publications have reported on the importance of the humidity for ionic conductivities [31, 32], as well as the interesting behavior of ions in polyelectrolyte multilayers and polyelectrolyte complexes [33]. These results clearly reveal that a full understanding can be only achieved by novel theoretical insights into the underlying mechanism. Recent computer simulation results for polyethylene oxide/Li+ mixtures, and the corresponding validated broad diversity of transport mechanisms, may indicate that the present view has to be eventually refined [34].

In this paper, we investigate the solvation properties of the aforementioned sulfonated polyelectrolytes and the corresponding ionic condensation behavior. We specifically focus on the consequences of polar and apolar solvents on the corresponding cation condensation constants. Our results indicate a significant dependence of the ion condensation behavior on the preferential binding coefficient. It will be shown that the presence of DMSO leads to low ionic condensation constants, while the results for water and chloroform are more pronounced. We have further estimated the values for the sodium conductivities. Our findings reveal that high values for the diffusion constants are of the same importance as the corresponding low condensation constants to yield high sodium conductivities. Furthermore, we have investigated the polyelectrolyte conformations in dependence of the surrounding solvent. Although we have investigated a specific class of polyelectrolytes, it can be concluded that the results are generally valid for macromolecules that contain highly charged, polar and apolar groups.

The paper is organized as follows. In section 2 we present the theoretical background, which is needed for the analysis of the solvation and condensation properties. The simulation method, the parameters and the molecular structures are presented in section 3. Section 4 presents the numerical results. We conclude and summarize in section 5.

2. Theoretical background

2.1. Kirkwood–Buff integrals and the preferential binding parameter

The evaluation of statistical mechanics methods on the solvent and ion distribution function allows important insights into the preferential binding behavior in terms of the corresponding Kirkwood–Buff theory, which was introduced in the early 1950s [35, 36]. The radial distribution function of molecules or atoms β around solutes α can be expressed by

$$g_{\alpha\beta}(r) = \frac{\rho_\beta(r)}{\rho_{\beta,\infty}}, \tag{1}$$

where $\rho_\beta(r)$ denotes the local density of β at a distance r around the solute, and $\rho_{\beta,\infty}$ is the global density in the bulk phase [37]. The integrated radial distribution function gives the cumulative number distribution function

$$f_{\alpha\beta}(r) = 4\pi \int_0^r g_{\alpha\beta}(r)\, \mathrm{d}r, \tag{2}$$

which yields an estimate for the number of molecules of type β within a radius r around molecule α [38]. The Kirkwood–Buff integral is given by the integration of equation (1)

$$G_{\alpha\beta} = \lim_{R\to\infty} G_{\alpha\beta}(R) = \lim_{R\to\infty} \int_{r=0}^{r=R} 4\pi r^2 (g_{\alpha\beta}(r) - 1)\, \mathrm{d}r, \tag{3}$$

where the above relation is valid in the limit of $R = \infty$ [35, 36, 39–41]. Due to the presence of a finite box length in computer simulations, one typically defines the radial Kirkwood–Buff parameter as

$$G_{\alpha\beta}(r) = \int_0^r 4\pi r^2 (g_{\alpha\beta}(r) - 1)\, \mathrm{d}r, \tag{4}$$

where the lower integration limit defines the molecular surface and the upper value is given at the point where the values of $G_{\alpha\beta}(r)$ converge [39, 40]. Equation (3) can be used to calculate the excess coordination number of atoms β (sodium ions) around α (polyelectrolyte) via [35, 36, 39–41]

$$N_\beta^{xs} = \rho_{\beta,\infty} G_{\alpha\beta} = \rho_{\beta,\infty} \lim_{R\to\infty} G_{\alpha\beta}(R), \tag{5}$$

which allows us to evaluate the preferential binding coefficient $\nu_{\beta\gamma}(R)$. Under the assumption of finite distances r, the radial preferential binding coefficient is given by

$$\nu_{\beta\gamma}(r) = \rho_{\beta,\infty}(G_{\alpha\beta}(r) - G_{\alpha\gamma}(r)) = N_\beta^{xs}(r) - \frac{\rho_{\beta,\infty}}{\rho_{\gamma,\infty}} N_\gamma^{xs}(r), \tag{6}$$

where the index γ represents solvent molecules (water, chloroform or DMSO), while α and β denote the polyelectrolyte and the sodium ions. A positive value for the preferential binding coefficient of equation (6) implies an energetically favorable binding of sodium ions [39, 40] due to

$$\Delta F_{\beta\gamma}^{\mathrm{t}}(r) = -RT\nu_{\beta\gamma}(r), \tag{7}$$

which illustrates the connection of the preferential binding coefficient with the transfer free energy $\Delta F_{\beta\gamma}^{\mathrm{t}}$ multiplied with the molar gas constant R and temperature T. The transfer free energy gives an estimate for the amount of energy that is needed to transfer a sodium ion from a point r to the close vicinity of the polyelectrolyte surface.

2.2. Binding free energy

Several methods have been proposed over the years ([37, 43, 44] and references therein) to obtain an estimate for the binding free energy between two species. It has been often discussed that the estimation of free energy differences is a challenging task in computer simulations. A well-defined sampling of the configurational space is mandatory. An easier option that is applicable for solvent–solute interactions is the estimation of the binding free energy $F(r)$ at the distance r between two species via the pair radial distribution function $g_{\alpha\beta}$ [37, 45]

$$\Delta F(r) = -k_{\mathrm{B}}T\ \log\left(g_{\alpha\beta}(r)\right) + C, \tag{8}$$

where the constant C is given by reference energy values. With the binding free energies, the solvation properties for different solvents can be estimated and solvophobic as well as solvophilic properties can be identified.

3. Molecular structures and numerical details

The all-atom molecular dynamics simulations have been conducted by using the GROMACS 4.5.5 package [46, 47]. The topology of the sulfonated polyelectrolyte (mod-s220 Na^+, as shown in figure 1), and the force field (GROMOS43A1 [49]) have been derived with the help of the PRODRG server [48] (http://davapc1biochdundeeacuk/prodrg/). It has to be noted, in contrast to a recent experimental study of s220 $(Li/Na)^+$ [5], that we fixed the position of the $-SO_3-$ group at the carbon 3 position in the phenyl ring. This specific structure allows us to investigate the solvation properties for identical monomers. To emphasize the difference to the experimentally studied structure of the s220$(Li/Na)^+$ [5], we will denote our simulated polyelectrolyte mod-s220 Na^+ in the following. The number of monomers was $n = 9$, which is comparable to the size of nearly identical subunits in recently developed block copolymers [10]. Two methyl groups form the end monomers of the polyelectrolyte. To achieve system electroneutrality, nine sodium ions were randomly placed in the simulation box.

We have performed our molecular dynamics simulations of the polyelectrolyte in explicit extended simple point charge water model (SPC/E) water [50], chloroform ($CHCl_3$) and DMSO ($((CH_3)_2S{=}O$) DMSO) solution whose topologies and force field parameters are included in the GROMOS53A6 force field [51]. The NVT simulations have been carried out under periodic boundary conditions. The box sizes had the dimensions of $(5.238\,53 \times 5.238\,53 \times 5.238\,53)\,nm^3$ for water (4691 molecules), $(8.118\,53 \times 8.118\,53 \times 8.118\,53)\,nm^3$ for DMSO (4756 molecules) and $(9.1 \times 9.1 \times 9.1)\,nm^3$ for the chloroform solution (4704 molecules). All values have been matched to the experimentally determined densities for the solvents at 300 K [52]. The corresponding sodium and monomer concentrations are given by $0.10\,mol\,l^{-1}$ for water, $0.03\,mol\,l^{-1}$ for DMSO and $0.02\,mol\,l^{-1}$ for the chloroform solution.

We have matched the values for λ for comparison, which defines the ratio of the number of solvent molecules to the number of sulfonate groups by $\lambda(\text{solvent}) = [\text{solvent}]/[-SO_3-]$ [5]. In regards to the aforementioned values for the number of solvent molecules, we obtain $\lambda(H_2O) = 521$, $\lambda(\text{DMSO}) = 528$ and $\lambda(\text{chloroform}) = 523$. Electrostatic interactions have been calculated by the particle mesh Ewald sum [53]. The time step was $\delta t = 2\,fs$ and the temperature was kept constant by a Nose–Hoover thermostat [42] at 300 K. All bonds have been constrained by the LINCS algorithm [54]. We performed a warm-up phase for 25 ns after energy minimization with the steepest descent method to ensure conformational equilibrium for the polyelectrolytes. The following production runs for each solvent have been conducted for 80 ns. Snapshots of the system were printed out with intervals of 2 ps.

The solvent accessible surface area Σ_{tot} was calculated by the sum of spheres centered at the atoms of the polyelectrolyte, such that a spherical solvent molecule can be placed at closest distance and in agreement to van-der-Waals interactions by following the constraint that other atoms are not penetrated [55]. The corresponding apolar Σ_- and polar solvent accessible surface area Σ_+ have been calculated by following the same procedure as for the total solvent accessible surface area, by taking into account only apolar and polar atoms, respectively. An atom was defined as polar if the partial charge was larger than $|0.2|e$. With regard to the underlying force field, the polar atoms of mod-s220 Na^+ are sulfur and oxygen atoms, whereas the carbon and hydrogen atoms are considered to be apolar.

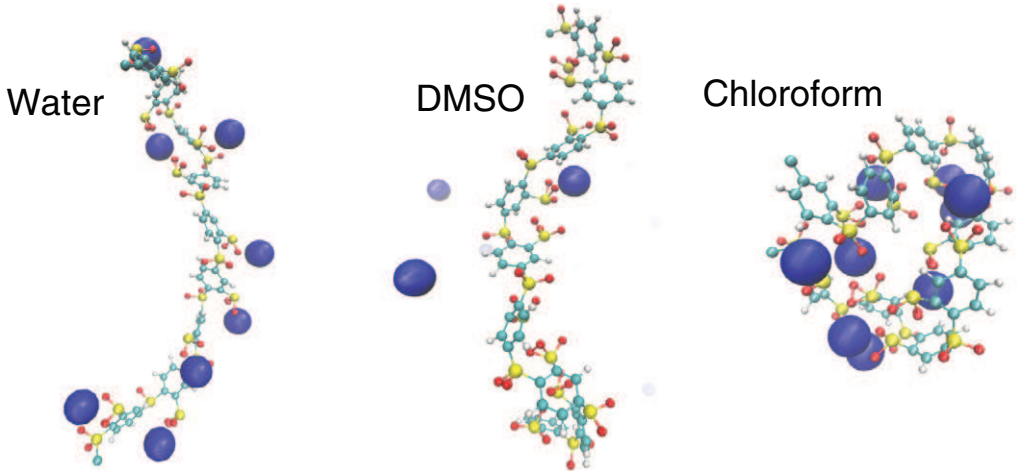

Figure 2. Simulation snapshots of mod-s220 Na^+ in water (left), DMSO (middle) and chloroform (right). The sodium ions are shown as blue spheres.

4. Simulation results

Typical simulation snapshots for conformations of mod-s220 Na^+ in water, DMSO and chloroform are presented in figure 2. At a first glance, it can be clearly seen that the presence of DMSO and water results in a significantly expanded conformation of mod-s220 Na^+ compared to the presence of chloroform, which leads to a strongly collapsed configuration. The dependence of the molecular shape on the polarity of the solution (experimental values: $\epsilon_{\text{water}} = 78$, $\epsilon_{\text{DMSO}} = 47$ and $\epsilon_{\text{chloroform}} = 2$) can be explained by the Flory–Huggins theory [56] if it is assumed that the polyelectrolyte conformation is mainly dominated by the presence of polar groups. Thus, for strongly varying dielectric constants, as given for the different solvents, one would expect different conformations for the polyelectrolyte in terms of favorable solvent–monomer interactions [56]. The situation is more complex if the chemical structure of the polyelectrolyte is explicitly taken into account. It is clear that the applicability of the Flory–Huggins theory is less obvious if apolar groups like the phenyl ring alternate with polar groups like the sulfone and the sulfonate groups [20]. Thus, the different regions expose more or less surface area in regards to the polarity of the solvent and the considered polyelectrolyte groups. To emphasize this point, it has to be mentioned that 57% of the polyelectrolyte atoms can be identified as hydrophobic (all atoms except sulfur and oxygen) with the corresponding definition as given in the last section. Hence, it can be concluded that the detailed chemical characteristics of the polyelectrolyte, as well as of the solvent, have to be taken into account to understand the conformation properties. This can also be seen by comparing the polyelectrolyte conformation between DMSO and water. Although the dielectric constants for water and DMSO differ around $\Delta\epsilon \approx 31$, the extended conformations in both solutions are nearly identical in their size. In regards to the counterion condensation behavior, the Bjerrum length $\lambda_B = e^2/4\pi\epsilon k_B T$ [57] with the elementary charge e and the thermal energy $k_B T$, which gives an estimate for the length scale where thermal and electric potential energy are identical, differs by a factor of 1.66 ($\lambda_B(H_2O) \approx 0.7$ nm and $\lambda_B(\text{DMSO}) \approx 1.16$ nm at 300 K). Thus, it can be assumed that the counterion condensation behavior is more pronounced for DMSO. As figure 2 illustrates, it can be recognized that this assumption fails. This fact is of further importance

Table 1. Radius of gyration R_g, end-to-end radius R_e, polar Σ_+, apolar Σ_- and total solvent accessible surface area Σ_t with standard deviations for mod-s220 Na^+ in different solvents.

Solvent	R_g (nm)	R_e (nm)	Σ_+ (nm^2)	Σ_- (nm^2)	Σ_t (nm^2)
Water	1.08 ± 0.14	2.42 ± 0.73	9.74 ± 0.50	6.54 ± 0.41	16.28 ± 0.83
DMSO	1.18 ± 0.04	3.32 ± 0.12	9.20 ± 0.17	7.26 ± 0.19	16.45 ± 0.26
Chloroform	0.65 ± 0.03	0.71 ± 0.27	6.22 ± 0.29	6.72 ± 0.25	12.94 ± 0.43

concerning the classical Manning–Oosawa counterion condensation theory [58–60], which explicitly states that the number of condensed counterions increases with the Bjerrum length. To investigate these points in more detail, and to clarify the observed characteristics, we will explicitly take into account the detailed chemical interactions between all species. We start our study by the investigation of the conformational properties for polyelectrolytes in different solvents.

4.1. Solvation properties for different solvents

To study the influence of different solvents on the conformational properties of the polyelectrolyte, we have determined the radius of gyration, the end-to-end distance and the solvent accessible surface area for mod-s220 Na^+. The radius of gyration R_g is given by

$$R_g^2 = \frac{1}{2n^2} \sum_{i,j}^{n} (\vec{R}_i - \vec{R}_j)^2, \tag{9}$$

where n denotes the number of monomers and $\vec{R}_i$, $\vec{R}_j$ the positions for different monomers i, j [56]. Another expression that can be used to estimate the conformational behavior is given by the end-to-end distance

$$R_e^2 = (\vec{R}_1 - \vec{R}_n)^2, \tag{10}$$

which connects the position of the first monomer $\vec{R}_1$ to the last monomer $\vec{R}_n$ [56]. The values for the different solvents are shown in table 1. It can be clearly seen that the average values for R_g and R_e are comparable for DMSO and water. Nevertheless, the values for water are more fluctuating in regards to a more-pronounced standard deviation. One reason for this behavior is the stronger fluctuation of the number of condensed counterions in the presence of water compared to DMSO and chloroform, as will be discussed in the next subsection. In comparison to the values for DMSO and water, it can be concluded that chloroform is a significantly poorer solvent for the polyelectrolyte. The reason for the significant increase of the polyelectrolyte size in DMSO and water can be related to favorable solvent–polyelectrolyte interactions in agreement with the Flory–Huggins theory [56].

The polarity of the solvent in terms of different dielectric constants and their influence on the polyelectrolyte conformation can be also investigated by the amount of the exposed polar solvent accessible surface area Σ_+, which is calculated by taking into account the solvent accessible surface areas of the sulfur and oxygen atoms. It can be seen in table 1 that Σ_+ becomes larger in the order $\Sigma_+(\text{water}) > \Sigma_+(\text{DMSO}) > \Sigma_+(\text{chloroform})$. The coincidence between the polarity of the solvent as given by the dielectric constant and the amount of the polar solvent

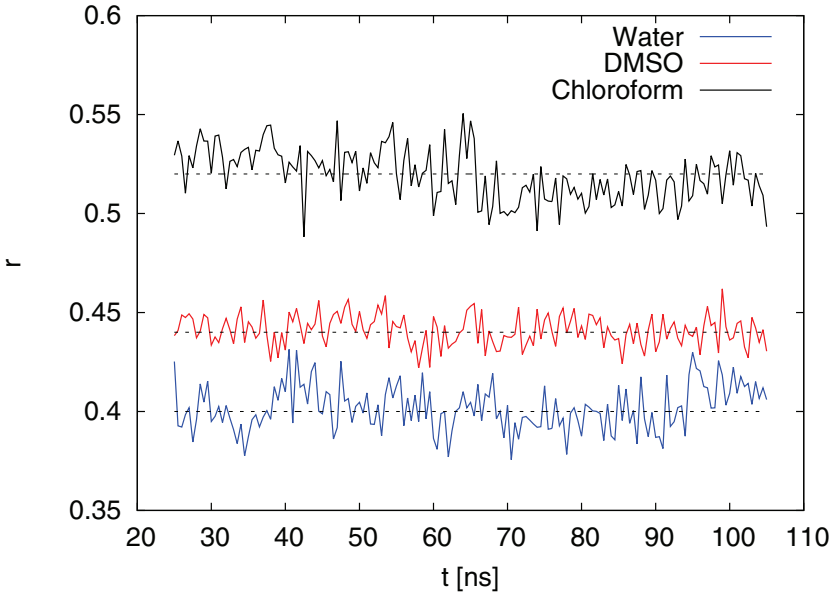

Figure 3. Ratio of the apolar to the total solvent accessible surface area $r = \Sigma_- / \Sigma_t$ for mod-s220 Na^+ in water, DMSO and chloroform during the simulated time scale. The dashed lines represent the average values as given in the text.

accessible surface area is obvious. In contrast, no trend can be recognized for the behavior of the apolar solvent accessible surface area Σ_- (all atoms except sulfur and oxygen) with respect to the polarity of the solvent. The order is given by Σ_-(DMSO)> Σ_-(chloroform) > Σ_-(water). This behavior indicates that the larger solvent accessible surface area of the polar groups in response to the polarity of the solvent is the main driving factor for extended configurations. Our results further evidence that the interactions of the polar groups with water are the most favorable ones, as can be seen by the largest polar solvent accessible surface area. In contrast, the large polarity of water avoids an interaction with the apolar groups, which explains the smaller values for the apolar solvent accessible surface area due to the hydrophobic effect [20]. Hence, the polyelectrolyte has to find a balance between the favorable and unfavorable exposed solvophilic and solvophobic solvent accessible surface area. We assume that the intermediate polarity of DMSO between water and chloroform, as given by the dielectric constant $\epsilon \approx 47$, favors a balanced increase in the polyelectrolyte size for the polar as well as the apolar groups, which results in the largest total solvent accessible surface area Σ_t compared to the other solvents.

The ratio of the apolar to the total solvent accessible surface area $R = \Sigma_- / \Sigma_t$ is shown in figure 3. It can be easily seen that the ratio R is significantly dependent on the polarity of the solvent. We have found values of $R(\text{water}) = 0.40 \pm 0.01$, $R(\text{DMSO}) = 0.44 \pm 0.01$ and $R(\text{chloroform}) = 0.52 \pm 0.02$. Thus, a decreased ratio of the apolar regions can be observed for polar solvents, which validates the presence of the solvophobic or hydrophobic effect. The opposite trend is also valid for the ratio of the polar to the total solvent accessible surface area by $R_- = 1 - R$. It becomes evident that the increase in the polyelectrolyte size is given by a subtle interplay between the apolar and polar regions of the polyelectrolyte and the corresponding response to the polarity of the solution. These findings are in good agreement with protein folding theory and the aggregation of hydrophobic particles, where it was assumed that the minimization of hydrophobic regions in terms of the hydrophobic collapse is the initial starting

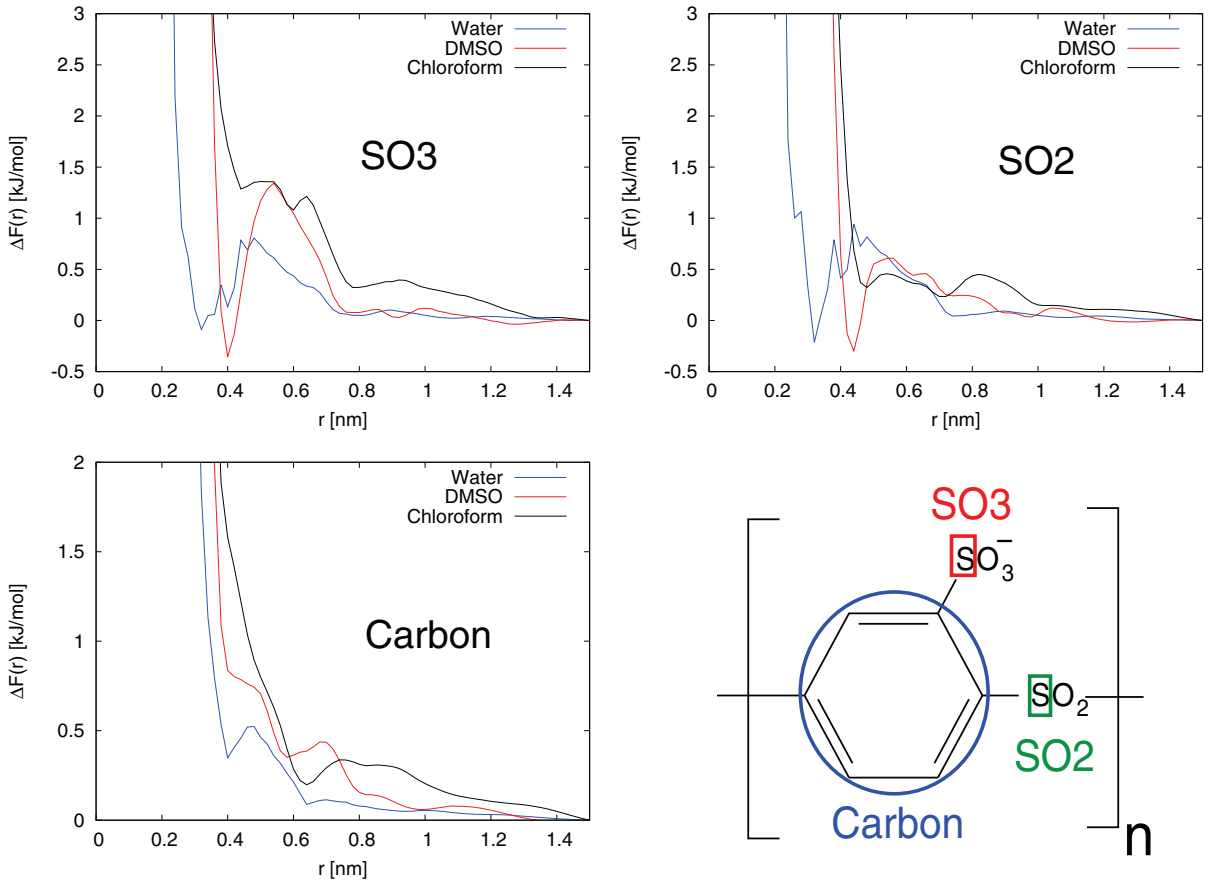

Figure 4. Binding free energy for solvent molecules around SO3 (top left), SO2 (top right) and carbon atoms (bottom left). The distance r is defined by the sulfur atom of the DMSO molecules, the carbon atom of the chloroform molecules and the oxygen atom of the water molecules, respectively, to the corresponding sulfur atoms and carbon atoms of mod-s220. All considered groups are indicated in the chemical formula (bottom right).

point for the formation of protein secondary and tertiary structures as well as self-aggregation of hydrophobic and amphiphilic molecules [19, 20].

Another important factor that influences the polyelectrolyte conformation is given by the number of condensed counterions. A strong condensation behavior corresponds to an efficient screening of electrostatic interactions between the charged groups, which results in weak repulsive forces between the monomeric charges [15, 61]. In regards to the qualitative results in figure 2, it can be seen that the largest number of condensed counterions occurs for chloroform followed by water. Obviously, the presence of DMSO leads to the smallest number of condensed sodium ions. Thus, the slightly more pronounced larger polyelectrolyte conformation size for DMSO, as given by the values of table 1, can be also related to stronger repulsive electrostatic interactions between the likewise charged $-SO_3-$ groups due to the smaller number of screened charges and the lower dielectric constant of the solvent. We will evaluate this point in the next section in more detail by the introduction of a quantitative analysis method.

The binding free energy between solvent molecules and the different polar and apolar groups is shown in figure 4. It can be clearly seen that DMSO leads to the strongest binding

behavior in the first solvation shell around the —SO_3— (SO3) group. The well-pronounced energetic minimum is located at 0.4 nm at the first solvation shell with an energy barrier of 1.5 kJ mol^{-1}, which prevents the release of solvent molecules to the second solvation shell at 0.8 nm. The binding energy compared to the bulk solution at 1.5 nm is negative with $\Delta F = -0.4$ kJ mol^{-1}, which indicates favorable interactions. The behavior for water is slightly different. The first energy minimum occurs at 0.3 nm with $\Delta F \approx -0.1$ kJ mol^{-1} and an energy barrier of roughly 0.8 kJ mol^{-1}. At this distance, most of the hydrogen bonds between the polyelectrolyte and water are present. The various small peaks within a distance of 0.3–0.45 nm can be related to different conformations of the water molecules around the SO3 group. In summary, it can be concluded that the overall binding energy of DMSO to the SO3 group is larger that of water. As was expected, the binding energy of chloroform is unfavorable for all distances due to the apolar properties of the solvent and the polar characteristics of the SO3 group. A nearly identical behavior to the SO3 group can be also observed for the SO2 group with less pronounced energy barriers and energy minima.

In addition, we have also analyzed the binding properties of the different solvents to the phenyl ring (carbon). It can be seen that the binding free energy is positive for all solvents. However, the most pronounced free energy minimum can be observed for chloroform at a distance of 0.6 nm. Hence, although the values are positive, the weakly pronounced affinity of association between apolar solvents and apolar groups becomes visible. In regards to the above-discussed results, it can be concluded that the molecular details of the polyelectrolyte solvent contact include a complex solvation mechanism due to alternating polar and apolar groups in the polyelectrolyte backbone. However, all estimated binding free energies are in good agreement with the above-discussed conformational behavior.

To further evaluate the binding properties of DMSO to the polyelectrolyte, we have calculated the spatial distribution of the solvent's center of mass for DMSO around an arbitrary middle monomer of the polyelectrolyte, as shown in figure 5. It can be clearly seen that a large fraction of DMSO molecules accumulates between the three sulfur-containing groups SO3 and SO2. It is further evident that DMSO molecules aggregate around the carbon ring and the SO3 group. Therefore, we assume that electrostatic interactions such as dipole–dipole interactions between DMSO and the partially charged groups of the polyelectrolyte are the main driving factor for the solvation properties of DMSO. For the investigation of the DMSO orientation, we have evaluated the radial distribution function $g_{S-C/O}$ between all sulfur atoms of the SO3 and SO2 groups and the corresponding carbon and oxygen atoms, respectively, of DMSO. The results are presented on the right side of figure 5. It can be clearly seen that a well-ordered orientation is given for the methyl groups (carbon atoms) of DMSO toward the sulfur atoms of the polyelectrolyte with the highest peak at 0.45 nm. It can be concluded that the DMSO molecules and specifically the slightly positively charged methyl groups and the central sulfur atom are electrostatically attracted by the oxygen atoms of the SO3 and SO2 groups. It has to be noted that the corresponding orientation analysis for water is not that well pronounced due to the larger number of condensed sodium ions that electrostatically interact with the solvent molecules. We will come back to this point in more detail in the next section.

We have further estimated the cumulative number distribution function of solvent molecules around the polyelectrolyte surface area according to equation (2), and have multiplied it with the molecular volume of the distinct solvent molecules, as shown in figure 6. The multiplication by the molecular volume allows us to take excluded-volume effects into account.

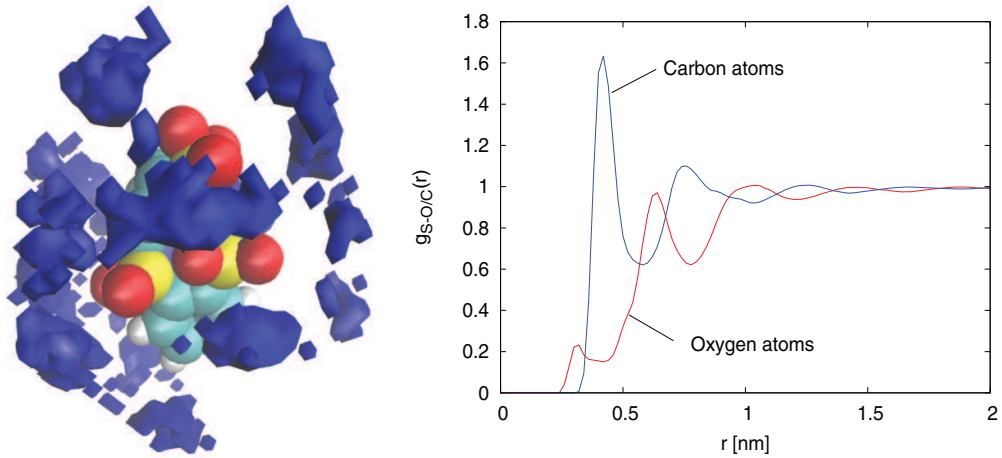

Figure 5. Left side: spatial distribution function of DMSO molecules (center-of-mass in dark blue) around arbitrarily chosen two middle connected monomers of mod-s220 up to a maximum distance of 0.8 nm from the macromolecular surface. The color legend is as follows: yellow, red, light blue and white denote sulfur, oxygen, carbon and hydrogen atoms, respectively. The sulfur–oxygen atoms on the left side of the molecule represent the SO2 group. The two other sulfur-containing groups represent SO3 groups. Right side: the radial distribution function between the sulfur atoms of the SO3 group and the carbon and oxygen atoms of DMSO.

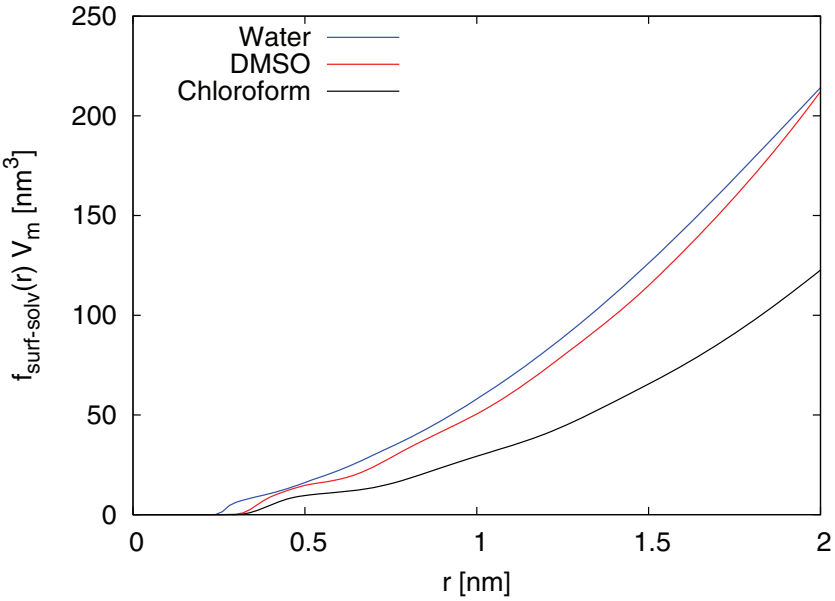

Figure 6. Cumulative number distribution function according to equation (2) between the surface of the polyelectrolyte and the solvent molecule position multiplied by molecular solvent volume V_m.

We have determined the molecular volumes of $V_m(\text{water}) \approx 0.065\,\text{nm}^{-3}$, $V_m(\text{DMSO}) \approx 0.217\,\text{nm}^{-3}$ and $V_m(\text{chloroform}) \approx 0.232\,\text{nm}^{-3}$. It can be clearly seen that DMSO and water occupy a larger volume around the polyelectrolyte compared to chloroform, which can be related to favorable interactions. After the first solvation shell for water and DMSO around 0.4 nm, it can be seen that DMSO and water have a nearly identical occupied volume. The main

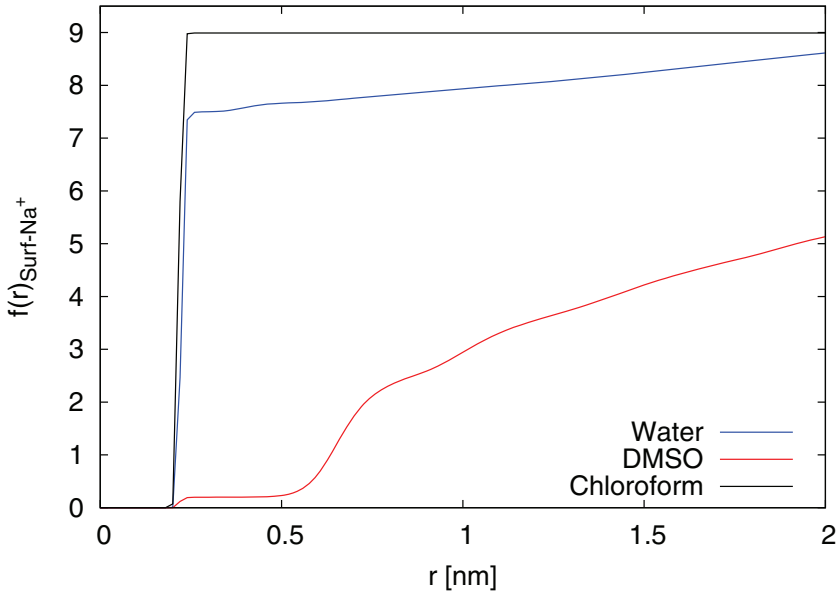

Figure 7. The cumulative number distribution function for sodium ions around the molecular surface of mod-s220 Na^+ for different solvents.

differences occur due to the ordering behavior in the second solvent shell of DMSO, as given for values around 0.6 nm. A strong depletion effect can be therefore observed for DMSO within a distance of 0.5–0.6 nm, which corresponds to the broad and pronounced transition and energy barrier, respectively, of the first to the second solvation shell in agreement with the results of figure 4.

4.2. Ionic condensation behavior for different solvents

As we have shown qualitatively in figure 2, the ionic condensation behavior increases for the case where DMSO < water < chloroform. This observation is validated by figure 7, where the cumulative number distribution function of sodium ions around the polyelectrolyte surface according to equation (2) is shown. We have identified the fraction of condensed sodium ions by considering the number of ions within the corresponding Bjerrum length. A nearly full association of sodium ions around mod-s220 Na^+ can be observed in the presence of chloroform. Due to the apolar character of chloroform, the counterions tend to associate with the charged polyelectrolyte groups. In addition, the very large Bjerrum length of $\lambda_B \approx 25$ nm, due to the low dielectric constant in the chloroform solution, leads to strong association properties. The observed behavior for chloroform can be explained by the Manning–Oosawa counterion condensation theory [58–60, 62]. It was originally proposed that counterion condensation occurs if $\Gamma = \lambda_B / l_c \gg 1$ where l_c is the distance between two neighboring charged polyelectrolyte groups. For chloroform, it is clearly evident that $\Gamma \gg 1$, which results in the presented behavior.

The situation is less clear if the condensation behavior for DMSO and water is considered. Figure 7 significantly illustrates that more ions are condensed in the presence of water compared to DMSO, although $\Gamma_{water} < \Gamma_{DMSO}$ due to a smaller water Bjerrum length. If we calculate the fraction of condensed counterions by dividing the number of counterions within the distance of the Bjerrum length N_{λ_B} with the total number of counterions N in terms of $r_c = N_{\lambda_B}/N$,

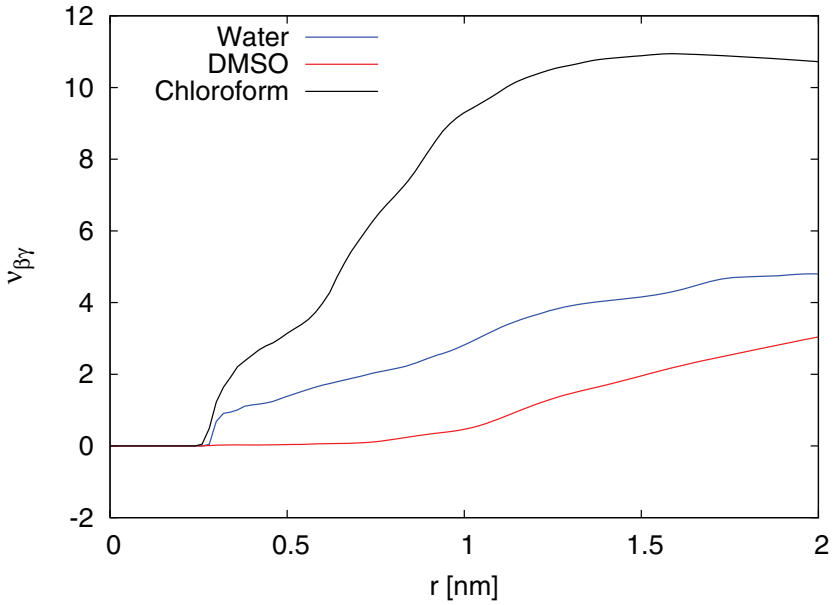

Figure 8. The radial preferential binding coefficient $\nu_{\beta\gamma} = -\Delta F^t_{\beta\gamma}/RT$ according to equation (7) for sodium ions and their binding to the SO3 group in the polyelectrolyte. The values for the radial distribution function have been evaluated with regard to the sulfur atoms in the polyelectrolyte.

we derive a condensation constant of $r_c \approx 0.86$ for water, while DMSO leads to a constant of $r_c \approx 0.38$ (chloroform $r_c = 1$). The low condensation constant for DMSO may also explain the larger polyelectrolyte conformation size compared to water due to unscreened repulsive electrostatic interactions between the SO3 groups, as was discussed above. Furthermore, it has to be remarked that the number of condensed counterions in water is strongly fluctuating, as has been observed in the larger standard deviations compared to DMSO and chloroform. As a consequence, we can relate this effect to the larger fluctuations of the radius of gyration and end-to-end distance as were shown in table 1.

A main driving force for the ionic condensation behavior is given by the counterion binding free energy, which can be also expressed by the transfer free energy according to equation (7). The affinity for association at each distance can be calculated by the radial preferential binding coefficient $\nu_{\beta\gamma}(r)$ according to equation (6). The corresponding radial distribution functions have been evaluated by taking into account the sulfur atom of the SO3 group and the corresponding centers of masses for the solvent molecules and sodium ions, respectively. The values for the radial preferential binding coefficient are shown in figure 8. It can be clearly seen that the preferential binding coefficient is positive for all distances and solvents. This indicates that the transfer of ions from the bulk solution to the polyelectrolyte surface according to equation (7) is a favorable process. It becomes obvious that the transfer free energy for chloroform is roughly 4 times and 2.5 times, respectively, more favorable compared to DMSO and water. These large values clearly indicate that free counterions in chloroform are nearly absent in agreement with the above-discussed results. It can be additionally seen that the association of sodium ions around the polyelectrolyte in an aqueous solution is more favorable compared to DMSO, which is in agreement with the determined higher condensation constant r_c for water. This behavior has been also experimentally validated [63], where it was found

that the transfer free energy of a sodium ion from an aqueous solution to DMSO is negative. With regards to these results, we conclude that the pronounced deviations in the ionic solvation properties for DMSO and water are responsible for the different observed ionic condensation constants.

The detailed solvation behavior for the sodium ions can be evaluated in terms of the pair radial distribution function, as shown in figure 9. We have considered all sodium ions within a distance of 0.7 nm of the macromolecular surface, as condensed to the polyelectrolyte. It can be clearly seen that the number of water molecules in the first hydration shell, up to a distance of 0.32 nm, differs for condensed and free sodium ions. This can be mainly explained by the close distance to the polyelectrolyte in terms of steric interactions. We have further evaluated the cumulative number distribution function by the corresponding evaluation of the pair radial distribution functions according to equation (2), to determine the number of solvent molecules in the first shell. The corresponding results at 0.32 nm are given by $N_c = 5.45 \pm 0.02$ water molecules for free sodium ions and $N_c = 4.53 \pm 0.14$ water molecules for condensed sodium ions. The results for the free ions are in good agreement to a recent publication where this number has been determined to be around $N_c = 5.7$–5.8 [64]. Furthermore we have also evaluated the corresponding binding free energies of sodium ions to solvent molecules by using equation (8). Compared to the bulk solution at $r \geqslant 1$ nm where the radial distribution function converges, we have determined $\Delta F(\text{water, free}) \approx -4.2\,\text{kJ mol}^{-1}$ for the free ions and $\Delta F(\text{water, condensed}) \approx -3.3\,\text{kJ mol}^{-1}$ for the condensed ions. The corresponding analysis for DMSO (the middle sketch of figure 9) shows that there is really a negligible difference in the solvation behavior for condensed and free sodium ions in DMSO. It can be assumed that a full solvation shell is always around the sodium ions, which indicates the good solubility of sodium in DMSO. This is also clearly evidenced by the large binding free energies of condensed and free ions with $\Delta F(\text{DMSO, free/condensed}) \approx -5.3\,\text{kJ mol}^{-1}$, which is around $1\,\text{kJ mol}^{-1}$ more favorable compared to water. If the number of DMSO molecules in the first solvation shell, up to a distance of 0.42 nm, is analyzed, we find nearly identical values for condensed and free ions with $N_c = 5.97 \pm 0.02$ and 5.99 ± 0.02 DMSO molecules. These values are in qualitative agreement with literature results, which have been estimated by *ab initio* methods [65]. As a reason for the good solubility, it has been emphasized that the solvation properties of sodium ions in DMSO are extremely well pronounced. DMSO can be considered as a coordinating solvent in terms of significant electron pair donor abilities [66]. These properties can be also expressed by the so-called donor numbers [66, 67], which give an estimate of the solubility of an ion in a specific solvent. The donor numbers for water and DMSO are given by $\text{DN}_{\text{H}_2\text{O}} = 18\,\text{kcal mol}^{-1}$ and $\text{DN}_{\text{DMSO}} = 29.8\,\text{kcal mol}^{-1}$, whereas chloroform shows a vanishing donor number [67] in agreement with our findings with regard to the condensation properties.

It is evident that there is a strong difference in the solvation behavior for condensed and free sodium ions in chloroform, despite the low statistical accuracy due to the small number of free counterions at distances $r \geqslant 0.6$ nm. We have identified values of $N_c = 5.63 \pm 0.18$ chloroform molecules for free, and $N_c = 3.21 \pm 0.14$ chloroform molecules for condensed sodium ions. The binding energy is smallest compared to DMSO and water, and has been estimated to $\Delta F(\text{chloroform, free}) \approx -1.1\,\text{kJ mol}^{-1}$ for the free ions and $\Delta F(\text{water, condensed}) \approx -0.2\,\text{kJ mol}^{-1}$ for the condensed ions. Hence the small values for the binding free energy clearly indicate the poor solubility of sodium ions in a chloroform solution, which may also result in the large condensation constant for this solvent and which is in agreement with the donor number concept [67].

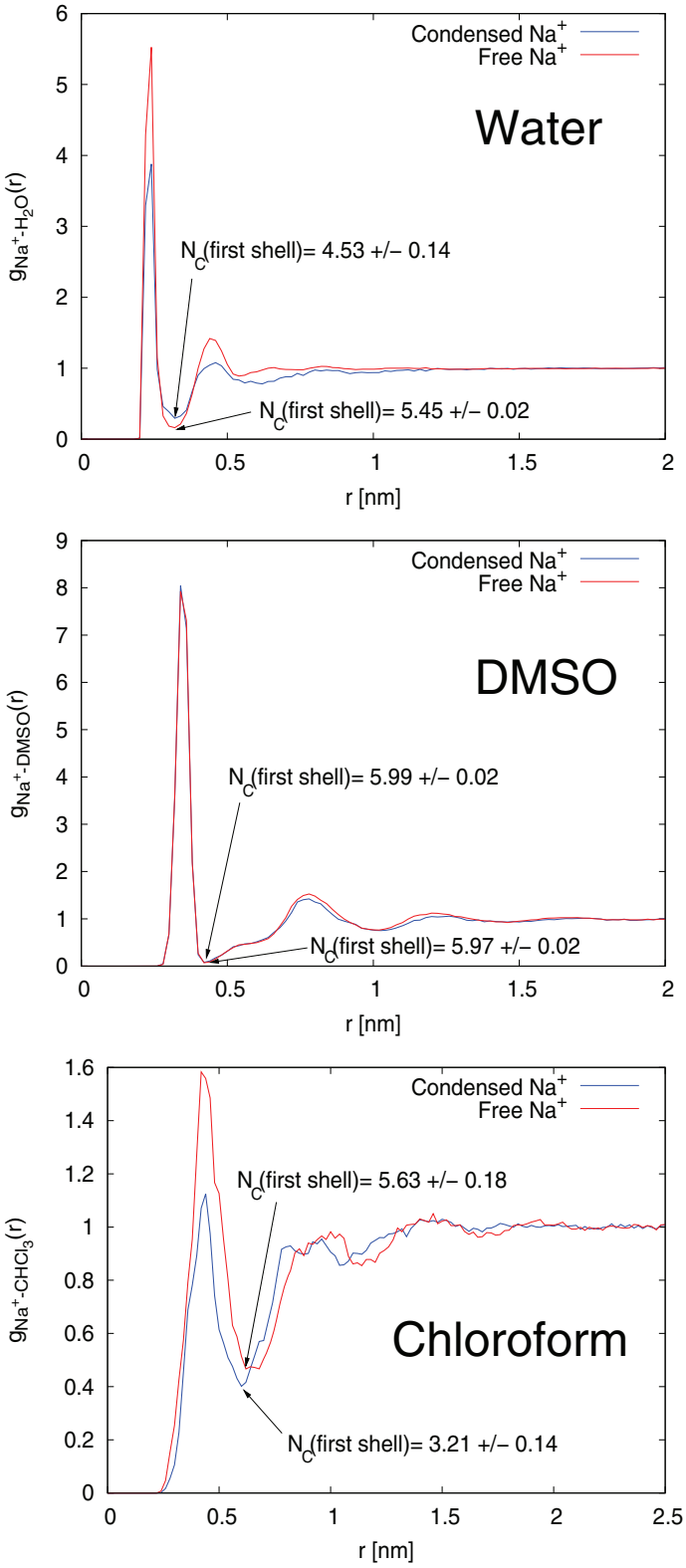

Figure 9. Pair radial distribution function $g_{\mathrm{Na^+-solv}}(r)$ for solvent molecules (centers-of-mass) around the sodium ions for water (top), DMSO (middle) and chloroform (bottom) divided into free (red line) and condensed (blue line) counterions.

Table 2. Sodium and solvent diffusion constants D_{Na^+} and D_s and sodium conductivity σ_{Na^+} in DMSO and water as calculated by equations (11) and (12).

Solvent	$D_{Na^+}(10^{-5}\,cm^2\,s^{-1})$	$D_s\,(10^{-5}\,cm^2\,s^{-1})$	$\sigma_{Na^+}\,(mS\,cm^{-1})$
Water	0.39 ± 0.01	2.71 ± 0.01	1.51 ± 0.01
DMSO	0.23 ± 0.01	0.74 ± 0.01	0.24 ± 0.01

4.3. Dynamic properties: diffusion constants and sodium conductivity

In this subsection, we present the dynamic behavior of the sodium ions in different solvents. Due to the fact that a nearly complete condensation of sodium ions in a chloroform solution has been validated, we purely restrict our analysis to water and DMSO. The sodium and solvent diffusion constants have been calculated via the mean-squared displacement [37, 42]

$$D = \lim_{t\to\infty} \frac{\langle(\vec{R}(t) - \vec{R}(t_0))^2\rangle}{6t}, \tag{11}$$

where $\vec{R}$ denotes the position of the sodium ions and the center-of-mass position for a solvent molecule at time t and t_0, respectively. The corresponding values are presented in table 2. It has to be noted that the calculated diffusion constant for the SPC/E water model is in excellent agreement with a previous publication [68]. The diffusion constants for DMSO are also in good agreement with additional results for united atom models [69, 70]. The comparison of the sodium diffusion constants between DMSO and water reveals that the value for water is roughly two times larger, in contrast to the pronounced difference between the solvent diffusion constants, which can also be explained by the larger condensation constant of sodium ions in an aqueous solution. In regards to a recent publication [5], it was proposed that the ionic dissociation constant can also be estimated by the ratio of the ion to the solvent diffusion constant via $r_{diss} = D_{Na^+}/D_s$. For the validity of this relation, it has to be assumed that the diffusion constant for solvated and dissociated ions roughly agrees with the solvent diffusion constant. A dissociation constant of $r_{diss} \approx 0.15$–0.2, which corresponds to a condensation constant of $r_{c,e} = 0.8$–0.85 for lithium ions in DMSO, has been estimated by the experiments for λ values around 8 [5]. As discussed in the last section, we have found a value for the sodium condensation constant of $r_{c,t} \approx 0.38$, which is significantly smaller than the experimental prediction. Following the approach presented in [5], we derive a dissociation constant for sodium ions in DMSO of $D_{Na^+}/D_s = 0.31$, which corresponds to a fictive condensation constant of 0.69. The difference between the differently derived condensation constants illustrates the fact that counterion condensation properties are hard to estimate by taking the diffusion constants into account.

An important estimator for the successful applicability of polyelectrolytes like mod-s220 Na^+ in technological products is given by the sodium conductivity σ. Although our simulated system is not directly comparable to experimental setups where a much higher counterion concentration is envisaged, an estimate for the ion conduction quality can be achieved by analyzing the simulation results. A reasonable option for determining the sodium conductivity in experiments and also for computer simulations is the usage of the Nernst–Einstein relation for cations [71]

$$\sigma_{Na^+} = \frac{Nq^2}{Vk_BT} D_{Na^+}, \tag{12}$$

where N is the number of sodium ions and $q = 1e$ the corresponding charge. The corresponding values are shown in table 2. Surprisingly, it can be seen that the sodium conductivity in water is roughly six times higher than DMSO, although the counterion condensation constant in water is larger. Therefore it can be concluded that a good choice for a solvent to optimize ionic and ion conductivities is given by the realization of large diffusion constants with a small ionic condensation constant.

5. Summary and conclusion

We have investigated the solvation properties of sulfonated small polyelectrolytes in different solvents via all-atom molecular dynamics simulations. Our main attention was devoted to the study of the static and dynamic properties as well as the ion condensation behavior in the different solvents DMSO, water and chloroform. All three solvents significantly differ in their polarity, as indicated by the corresponding dielectric constants.

We have validated that the polarity of the solvent strongly influences the amount of the polar and apolar solvent accessible surface area of the polyelectrolyte. Our results furthermore indicated that the presence of water leads to the largest ratio of the polar to the total solvent accessible surface area, followed by DMSO and chloroform in agreement with the polarity of the solution. We can relate this observation to the fact that macromolecules try to maximize their polar solvent accessible surface area in the presence of polar solvents, and vice versa for apolar solvents and apolar groups. The general consequences of this effect can seen in the famous hydrophobic collapse of proteins [19]. In regards to the specific alternating structure of polar and apolar groups, we have found that the largest polyelectrolyte conformation can be observed in the presence of DMSO, with an intermediate polarity compared to water and chloroform. This can be related to balanced contributions of favorable and unfavorable interactions, respectively, with polar and apolar polyelectrolyte groups. Thus, with regard to the observed differences in the dielectric constants, our results clearly demonstrate that for the considered solvents, solvation properties are more important than electrostatic interactions.

We have further evaluated the binding free energies between all three main groups of the polyelectrolyte and the solvent. The polar groups SO3 and SO2 have a negative binding free energy to DMSO and water. To emphasize the strong solvation properties of water and DMSO, we have further calculated the occupied molecular solvent volume around the polyelectrolyte, which is significantly larger for both solvents compared to chloroform. Therefore, we can conclude that water and DMSO are good solvents whereas chloroform can be interpreted as a poor solvent for the considered polyelectrolyte. These results are in good agreement with the observed radii of gyration and with recent experimental results where it has been found that the polyelectrolyte is nearly insoluble in chloroform [72].

Furthermore, we have evaluated the ionic condensation constants for all solvents. Interestingly, we have found that the presence of DMSO results in the smallest condensation constant compared to water and chloroform. This result is in disagreement with standard Manning–Oosawa counterion condensation theory, where a stronger counterion condensation is predicted for lower solvent dielectric constants. We were able to show that a rough estimate for the ionic condensation behavior is given by the evaluation of the preferential binding coefficient, which takes into account specific chemical details of the solvent. These results clearly reveal that electrostatic interactions are not the only factor to determine the counterion

condensation properties. Moreover, the specific chemical properties of the solvent in terms of solvation free energies and electron pair donor abilities [66, 67] have to be taken additionally into account.

Finally, we have also calculated the diffusion constants and the sodium conductivities in different solvents. Although the condensation constants are significantly smaller for DMSO, we have found a six times lower sodium conductivity compared to water, which is in qualitative agreement with recent experimental values [5]. Thus, it can be assumed that an increase of the diffusion coefficients by using small molecular weight solvents in combination with a high donor number is a reasonable option for increasing ionic conductivities.

In regards to the above-discussed results, we can conclude that solvation is a complex process that depends on the polarity of the solvent and the solvated molecular groups. Weak ionic condensation constants can be achieved by a balanced interplay between attractive electrostatic interactions in terms of high dielectric constants as well as good ionic solvation properties. The optimization of ionic conductivities as one of the main technological goals can be therefore achieved by a deeper understanding of the solvation processes and the underlying dynamic behavior. Our results clearly indicate that the specific chemical nature of the polyelectrolyte, the solvent and the ions have to be taken into account for a more reliable comparison with experimental results. The further development of polarizable atomistic force fields for macromolecules like AMOEBA [73] as well as force fields like ReaxFF [74] that could model the dissociation process would also certainly lead to novel insights into counterion or proton dissociation behavior and the electronic properties for polyelectrolytes in general. As a first step toward these new investigations, we have focused on the solvation properties and condensation behavior for a specific polyelectrolyte and its sodium counterions. We are confident that the variation of the solvent will be a good starting point for a deeper understanding of the chemical properties for polyelectrolytes in solution and the corresponding usage as ion conducting materials.

Acknowledgments

The authors have benefited from extensive and enlightening discussions with Klaus-Dieter Kreuer, Diddo Diddens and Andreas Heuer. Financial support is gratefully acknowledged by the Deutsche Forschungsgemeinschaft through the SimTech cluster of excellence and the SFB 716.

References

[1] Kreuer K-D (ed) 2013 *Fuel Cells, Selected Entries from the Encyclopedia of Sustainability Science and Technology* (Berlin: Springer)
[2] Hickner M A, Ghassemi H, Kim Y S, Einsla B R and McGrath J E 2004 *Chem. Rev.* **104** 4587
[3] Higashihara T, Matsumoto K and Ueda M 2009 *Polymer* **50** 5341
[4] Schwenzer B, Zhang J, Kim S, Li L, Liu J and Yang Z 2011 *ChemSusChem.* **4** 1388
[5] Kreuer K-D, Wohlfarth A, de Araujo C C, Fuchs A and Maier J 2011 *ChemPhysChem* **12** 2588
[6] Kreuer K-D, Paddison S J, Spohr E and Schuster M 2004 *Chem. Rev.* **104** 4637
[7] Schuster M, Kreuer K-D, Andersen H-T and Maier J 2007 *Macromolecules* **40** 598
[8] Schuster M, de Araujo C C, Atanasov V, Andersen H T, Kreuer K-D and Maier J 2009 *Macromolecules* **42** 3129

[9] de Araujo C C, Kreuer K-D, Schuster M, Portale G, Mendil-Jakani H, Gebel G and Maier J 2009 *Phys. Chem. Chem. Phys.* **11** 3305
[10] Titvinidze G, Kreuer K-D, Schuster M, de Araujo C C, Melchior J P and Meyer W H 2012 *Adv. Funct. Mater.* **22** 4456
[11] Wang C and Paddison S J 2013 *J. Phys. Chem.* A **117** 650
[12] Grady B P 2008 *Polym. Eng. Sci.* **48** 1029
[13] Smitha B, Sridhar S and Khan A A 2005 *J. Membr. Sci.* **259** 10
[14] Pawlak Z and Bates R G 1975 *J. Solut. Chem.* **4** 817
[15] Dobrynin A V and Rubinstein M 2005 *Prog. Polym. Sci.* **30** 1049
[16] Dobrynin A V, Rubinstein M and Obukhov S P 1996 *Macromolecules* **29** 2974
[17] Holm C, Limbach H J and Kremer K 2003 *J. Phys.: Condens. Matter* **15** S205
[18] Limbach H J, Holm C and Kremer K 2002 *Europhys. Lett.* **60** 566
[19] Ball P 2008 *Chem. Rev.* **108** 74
[20] Tanford C 1973 *The Hydrophobic Effect—Formation of Micelles and Biological Membranes* (New York: Wiley-Interscience)
[21] Rodnikova M N 2007 *J. Mol. Liq.* **136** 211
[22] Pace C N, Trevino S, Prabhakaran E and Scholtz J M 2004 *Phil. Trans. R. Soc.* B **359** 1225
[23] Yaacobi M and Ben-Naim A 1974 *J. Phys. Chem.* **78** 175
[24] Waigh T A, Ober R and Williams C E 2001 *Macromolecules* **34** 1973
[25] Qin Y and Fichthorn K A 2006 *Phys. Rev.* E **74** 020401
[26] van der Vegt N F A and van Gunsteren W F 2004 *J. Phys. Chem.* B **18** 1056
[27] Karpenko-Jereba L V, Kelterera A, Ninel P, Berezinab A and Pimenov V 2013 *J. Mem. Sci.* **444** 127
[28] Nomula S and Cooper S L 2001 *Macromolecules* **34** 925
[29] Schiessel H and Pincus P 1998 *Macromolecules* **31** 7953
[30] Wohlfarth A 2012 Talk held at the *Electrochemical Conference (Prague)*
[31] Cramer C, De S and Schönhoff M 2011 *Phys. Rev. Lett.* **107** 028301
[32] Akgöl Y, Cramer C, Hoffmann C, Karatas Y, Wiemhöfer H-D and Schönhoff M 2010 *Macomolecules* **43** 7282
[33] Schönhoff M, Imre A W, Bhide A and Cramer C 2010 *Z. Phys. Chem.* **224** 1555
[34] Maitra A and Heuer A 2007 *Phys. Rev. Lett.* **98** 227802
[35] Kirkwood J G and Buff F P 1951 *J. Chem. Phys.* **19** 774
[36] Ben-Naim A 1992 *Statistical Thermodynamics for Chemists and Biochemists* (New York: Plenum)
[37] Leach A 2001 *Molecular Modeling: Principles and Applications* (New York: Prentice-Hall)
[38] Smiatek J, Harishchandra R K, Rubner O, Galla H-J and Heuer A 2012 *Biophys. Chem.* **160** 62
[39] Yu I, Jindo Y and Nagaoka M 2007 *J. Phys. Chem.* B **111** 10231
[40] Baynes B M and Trout B L 2003 *J. Phys. Chem.* B **107** 14058
[41] Horinek D and Netz R R 2011 *J. Phys. Chem.* A **115** 6125
[42] Frenkel D and Smit B *Understanding Molecular Simulation* (San Diego, CA: Academic)
[43] Smiatek J and Heuer A 2011 *J. Comput. Chem.* **32** 2084
[44] Roux B 1995 *Comput. Phys. Commun.* **91** 275
[45] Smiatek J, Wagner H, Hentschel C, Chi L, Studer A and Heuer A 2013 *J. Chem. Phys.* **138** 044904
[46] Pronk S *et al* 2013 *Bioinformatics* **29** 845
[47] Hess B, Kutzner C, van der Spoel D and Lindahl E 2008 *J. Chem. Theor. Comput.* **4** 435
[48] Schüttelkopf A W and van Aalten D M F 2004 *Acta Crystallogr.* D **60** 1355
[49] van Gunsteren W F, Billeter S R, Eising A A, Hünenberger P H, Krueger P, Mark A E, Scott W R P and Tironi I G 1996 *Biomolecular Simulation: The GROMOS96 Manual and User Guide* (Zürich: Vdf Hochschulverlag)
[50] Berendsen H J C, Grigera J R and Straatsma T P 1987 *J. Phys. Chem.* **91** 6269
[51] Oostenbrink C, Villa A, Mark A E and van Gunsteren W F 2004 *J. Comput. Chem.* **25** 1656
[52] Lange N A and Dean A J 1973 *Lange's Handbook of Chemistry* (New York: McGraw-Hill)

[53] Darden T, York D and Pedersen L 1993 *J. Chem. Phys.* **98** 10089
[54] Hess B, Bekker H, Berendsen H J C and Fraaije J G E M 1997 *J. Comput. Chem.* **18** 1463
[55] Eisenhaber F, Lijnzaad P, Argos P, Sander C and Scharf M 1995 *J. Comput. Chem.* **16** 273
[56] de Gennes P G 1979 *Scaling Concepts in Polymer Physics* (Ithaca, NY: Cornell University Press)
[57] Russel W B, Saville D A and Schowalter W R 1989 *Colloidal Dispersions* (New York: Cambridge University Press)
[58] Manning G S 1969 *J. Chem. Phys.* **51** 924
[59] Oosawa F 1971 *Polyelectrolytes* (New York: Marcel Dekker)
[60] O'Shaugnessy B and Yang Q 2005 *Phys. Rev. Lett.* **94** 048302
[61] Dobrynin A V, Colby R H and Rubinstein M 1995 *Macromolecules* **28** 1859
[62] Holm C, Hofmann T, Joanny J F, Kremer K, Netz R R, Reineker P, Seidel C, Vilgis T A and Winkler R G 2004 *Adv. Polym. Sci.* **166** 67
[63] Krishnan C V and Friedman H L 1969 *J. Phys. Chem.* **73** 3934
[64] Rowley C N and Roux B 2012 *J. Chem. Theory Comput.* **8** 3526
[65] Westphal E and Pliego J R Jr 2005 *J. Chem. Phys.* **123** 074508
[66] Reichardt C and Welton T 2011 *Solvents and Solvent Effects in Organic Chemistry* (Weinheim: Wiley-VCH)
[67] Gutmann V 1976 *Coord. Chem. Rev.* **18** 225
[68] Mark P and Nilsson L 2001 *J. Phys. Chem.* A **105** 9954
[69] Vishnyakov A, Lyubartsev A P and Laaksonen A 2001 *J. Phys. Chem.* A **105** 1702
[70] Liu H, Müller-Plathe F and van Gunsteren W F 1995 *J. Am. Chem. Soc.* **117** 4363
[71] Schröder C and Steinhauser O 2008 *J. Chem. Phys.* **128** 224503
[72] Wohlfarth A and Kreuer K-D 2014 in preparation
[73] Ponder J W *et al* 2010 *J. Phys. Chem.* B **114** 2549
[74] van Druin A C T, Dasgupta S, Lorant F and Goddard III W A 2001 *J. Phys. Chem.* A **105** 9396